

Dual-Color Fluorescence Fluctuation Spectroscopy To Study the Complexation between Poly-L-lysine and Oligonucleotides

B. Lucas, E. Van Rompaey, S. C. De Smedt,* and J. Demeester

Laboratory of General Biochemistry and Physical Pharmacy, Ghent University,
Harelbekestraat 72, 9000 Ghent, Belgium

P. Van Oostveldt

Laboratory of Biochemistry and Molecular Cytology, Ghent University,
Coupure Links 653, 9000 Ghent, Belgium

Received February 14, 2002; Revised Manuscript Received June 24, 2002

ABSTRACT: In this study, dual-color fluorescence fluctuation spectroscopy (FFS) was explored to characterize the association of oligonucleotides (ONs) to cationic polymers. The results from dual-color FFS, in which both the ONs and the cationic polymers were fluorescently labeled, were compared with data obtained from single-color FFS in which only the ONs or the cationic polymers were fluorescently marked. As a model, the association of negatively charged 20-mer ONs to positively charged poly-L-lysine (pLL) was studied. The binding of rhodamine green-labeled ONs (RhGr-ONs) to nonlabeled pLL could be clearly observed in the fluorescence fluctuation profiles. Especially, highly intense fluorescence peaks appeared in the fluorescence fluctuations. A highly intense fluorescence peak was considered to originate from one complex in which a number of RhGr-ONs were present. Complexing nonlabeled ONs to rhodamine green-labeled pLL (RhGr-pLL) also resulted in highly intense fluorescence peaks, indicating not only that the complexes consisted of a number of ONs but also that numerous RhGr-pLL chains were present. Upon complexation of red-labeled pLL (Cy5-pLL) to green-labeled ONs (RhGr-ONs), highly intense fluorescence peaks occurred simultaneously in the red and green detector. These data proved the multimolecular composition of the polyplexes and agreed with the observations from single-color FFS.

Introduction

Ten years ago, antisense oligonucleotides were developed for the selective inhibition of various genes,¹ and more recently double stranded RNA is found to initiate sequence-specific gene silencing in mammalian cells.² Several laboratories have been encouraged to look for appropriate pharmaceutical carrier systems for ONs, as their cellular uptake is limited. Different types of cationic lipids and cationic polymers are under investigation to solve problems of hydrophilicity, size, negatively charged backbone, and nuclease sensitivity.^{3,4} Cationic lipids as well as cationic polymers spontaneously form soluble interpolyelectrolyte complexes with negatively charged nucleic acids, called respectively lipoplexes and polyplexes.⁵ The physicochemical features that govern the biological activity of lipo- and polyplexes are not well understood, partly due to the complexity of the association and dissociation behavior of such complexes. Indeed, a critical step in the delivery of ONs is the dissociation of the ONs from the complexes at the right place; i.e., in the cytoplasm of the target cell.⁶ If the affinity between the ONs and the cationic carriers is too low, the complex will dissociate prematurely, e.g., when it is still in the bloodstream or in the extracellular environment, while a strong affinity might prevent the release of the ONs intracellularly. A critical balance between “being associated extracellularly” and “being dissociated intracellularly” needs to be maintained.

Currently, the stability of DNA complexes is usually assessed using polyanion-disruption assays.^{7,8} Katayose

and Kataoka have studied the dissociation of poly(ethylene glycol)-poly-L-lysine/DNA complexes through the addition of poly(L-aspartic acid).⁹ However, to obtain real breakthroughs in the design and the understanding of the dissociation of DNA complexes *in cells*, there is an urgent need for advanced physicochemical methods, which allow characterizing this critical step in cells. Fluorescence fluctuation spectroscopy (FFS), which can be applied on a cellular scale,¹⁰ shows potential for that purpose. As illustrated in Figure 1A, FFS monitors the fluorescence fluctuations caused by the diffusion of fluorescent molecules through the excitation volume of a microscope. From the fluctuation profile (Figure 2A), an autocorrelation curve can be derived (Figure 2B) which allows calculating the diffusion coefficient of the fluorescent molecules. Expecting that the diffusion of the DNA will change upon release from its cationic carrier, one could extract information on the association and dissociation of interpolyelectrolyte complexes based upon their diffusion coefficient. With this idea in mind, our group has recently introduced *single-color* FFS in studying interactions between fluorescently labeled DNA and (nonlabeled) cationic polymers like poly(2-dimethylamino)ethyl methacrylate (pDMAEMA), poly(ethylenimine) (pEI), poly(ethylene glycol)-poly(ethylenimine) (pEG-pEI) and diamino-butane-dendrimer-(NH₂)₆₄ (DAB₆₄).^{11–13} We have shown, however, that autocorrelation analysis of the fluorescence fluctuation profiles of DNA/cationic polymer complexes is not feasible due to the presence of “highly intense fluorescence peaks” in the fluctuation profile (Figure 2C). The highly intense fluorescence peaks are explained by the migration through the excitation volume of “multimolecular” DNA/cationic polymer complexes, which are

* Corresponding author. Telephone: 0032-9-2648076. Fax: 0032-9-2648189. E-mail: stefaan.desmedt@rug.ac.be.

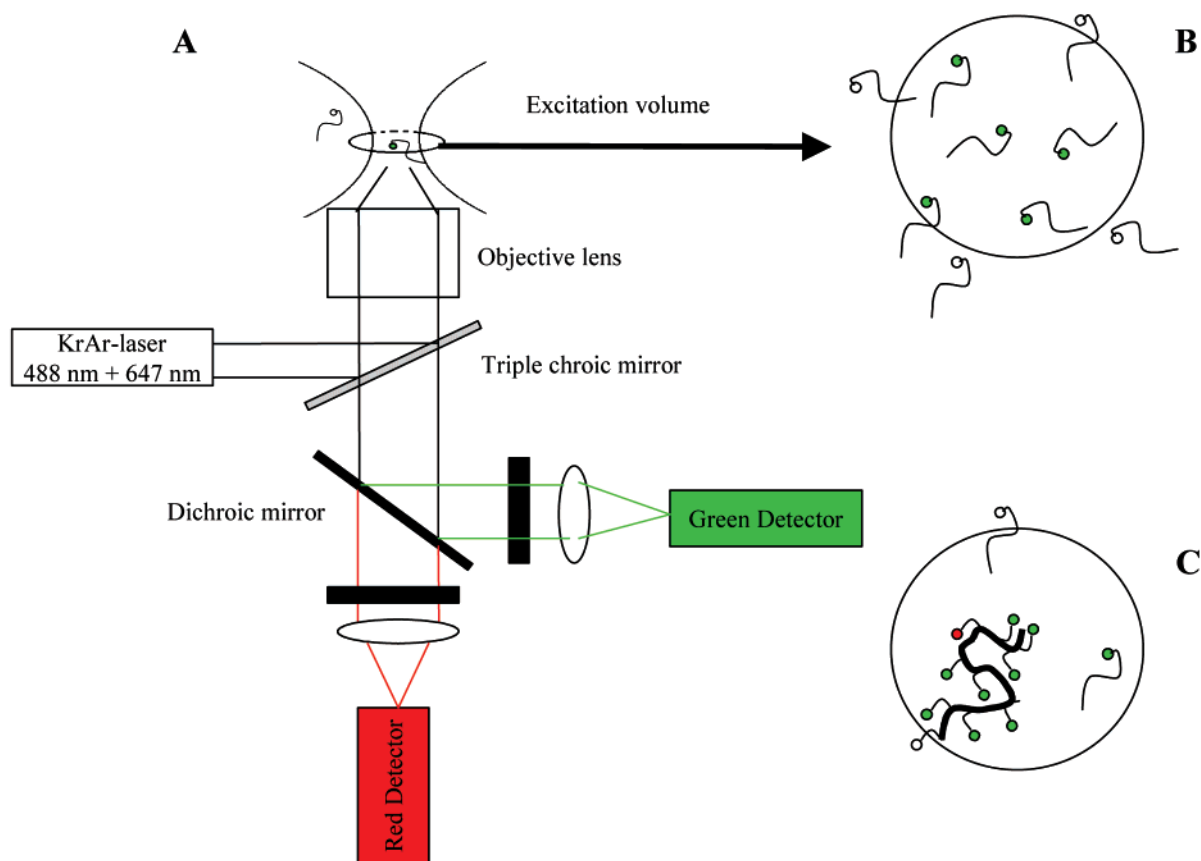


Figure 1. (A) Schematic setup of a FFS instrument. The excitation light from the laser is reflected by a triple chroic mirror into the back aperture of the objective lens. The light emitted by the fluorescent molecules in the excitation volume passes through the objective lens and the triple chroic mirror, to be split by the subsequent dichroic mirror into a red and a green component. (B) Schematic view of fluorescently labeled ONs, freely migrating through the excitation volume. Inside the excitation volume the fluorophores are excited and emit light (filled circles), outside the excitation volume the fluorophores remain in a dark ground state (open circle). (C) Schematic view of free fluorescently labeled ONs together with a very bright polymer/ON complex migrating through the excitation volume.

highly fluorescent as they carry a large number of fluorescently labeled ONs. We have concluded in this work that, in contrast to autocorrelation analysis, analyzing the fluorescence fluctuations by a method that distinguishes between species based upon their difference in fluorescence may allow the detection of associated and dissociated DNA.

To reveal how DNA/cationic carrier complexes physi-cochemically behave in cells, in many studies only the DNA is fluorescently marked. In some reports both the DNA and the cationic carrier are labeled with, spectrally different, fluorescent markers. Theoretically, fluorescence resonance energy transfer (FRET) between the fluorophore on the DNA and the fluorophore on the carrier could be a useful approach to study the complexation. However, FRET needs a proper orientation of the donor and acceptor molecules, which is hard to obtain in DNA/cationic carrier complexes. To also study the complexation of DNA/cationic carrier complexes in cells, dual-color microscopy has been proposed since it allows the simultaneous observation of the DNA and the cationic carrier in the cell.^{14–16} The colocalization of the fluorescent markers may indicate that the DNA and its carrier components are associated; a lack of colocalization may indicate that the DNA is released from its carrier. However, it remains possible that the fluorescent labeled molecules are colocalized without being associated. Compared with the spatial analysis of the fluorescently labeled molecules, the temporal

analysis of the movement of these molecules could be more robust to conclude whether the fluorescently labeled species are interacting. While dual-color microscopy answers the question “are they located together”, dual-color FFS may answer the question whether they move together. Moreover, compared with dual-color microscopy, dual-color FFS allows measurements at much lower concentrations of the molecules of interest.¹⁷

It has been shown recently that *dual-color* FFS allows the study of DNA hybridization, enzyme, and aggregation kinetics.^{18–21} Considering that dual-color FFS has never been used before for studying cationic polymer/DNA complexes, the present study aims to evaluate (1) whether the complexation between cationic polymers and ONs can be investigated by dual-color FFS and (2) whether the results revealed by dual-color FFS are consistent with the results obtained from single-color FFS. As a model, the *in vitro* complexation between a 20-mer ON and the polycation poly-L-lysine, which is intensively investigated as a pharmaceutical carrier for ONs,²² is considered.

Experimental Section

Oligonucleotides. The 20-mer phosphodiester ONs (5'-CCC-CCA-CCA-CTT-CCC-CTC-TC-3') (molar mass 5830 g/mol) and labeled analogues (using respectively rhodamine green and Cy5 as fluorescent markers) were synthesized by Euro-gentec (Seraing, Belgium). The fluorescent labeling occurred

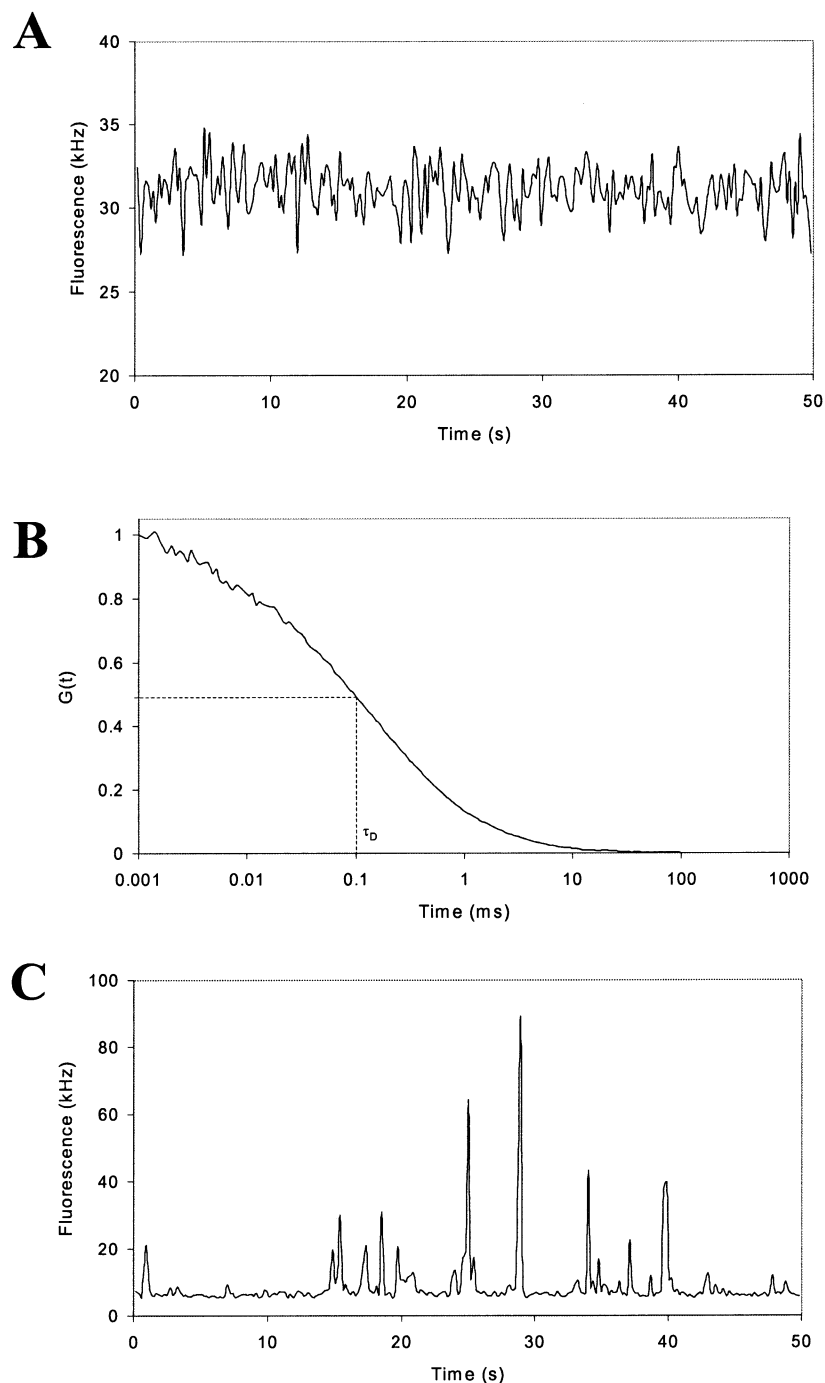


Figure 2. Fluorescence intensity profile (A) and corresponding autocorrelation function (B) of a solution of free fluorescent molecules, together with the fluorescence intensity profile of a mixture of free fluorescent molecules and bright complexes (C).

at the 5' end of the ONs; each oligonucleotide contained one label (RhGr or Cy5). The concentration of the ONs stock solutions (in Tris buffer at pH 8) was determined by absorption measurements at 260 nm ($1 \text{ OD}_{260} = 33 \mu\text{g ONs/mL}$). The contribution to the absorption at 260 nm by the label was taken into account in the determination of the concentration of the labeled ONs. The ONs stock solutions were further diluted with Hepes buffer (20 mM Hepes at pH 7.4).

Polymers. Poly-L-lysine was purchased from Sigma (St. Louis, MO). The molar mass, as determined from viscosimetric measurements, equaled 30 300 g/mol and was provided by the supplier. pLL stock solutions were prepared in Hepes buffer.

To prepare rhodamine green poly-L-lysine (RhGr-pLL), rhodamine green X-succinimidyl ester (RhGr-SE) was purchased from Molecular Probes (Eugene, OR). Poly-L-lysine was dissolved in "labeling buffer" (0.1 M NaHCO_3 at pH 8.8) at 1

mg/mL. To 1 mL of this pLL solution was added 50 μL of DMSO containing 0.13 mg of RhGr-SE drop by drop. After incubation for 1 h in the dark at ambient temperature, RhGr-pLL was purified on a G25-Sephadex column ($10 \times 100 \text{ mm}$), which was previously equilibrated with Hepes buffer. The fractions containing fluorescent pLL were collected. Finding of the amine concentration using the method of Snyder and Sobocinski²³ and measurement of the absorbance of the label allowed the determination of the average number of labels attached to the pLL. It could be calculated that, on the average, the pLL chains bore one RhGr-label.

Cy5-poly-L-lysine (Cy5-pLL) was prepared adding 1 mL of pLL solution (1 mg/mL in 0.1 M NaHCO_3 at pH 9.3) to a vial of FluoroLinkCy5 monofunctional dye (Amersham Pharmacia, Piscataway, NJ). After incubation for 1 h in the dark at ambient temperature, Cy5-pLL was purified as described

above. The degree of labeling was determined to be, on the average, one Cy5-label per pLL strand.

Dextran sulfate (DS) was purchased from Sigma (St. Louis, MO). The molar mass, provided by the supplier, equaled 500 000 g/mol. Stock solutions were prepared in Hepes buffer.

Preparation of Polyplexes. The pLL/ON complexes (varying in charge ratio (φ), see below) were prepared by adding (in one step) different volumes of the pLL stock solution to a fixed volume of the ONs stock solution. After addition of the polymer solution, the dispersion was vortexed for 10 s. To obtain the final ONs concentration of 10 $\mu\text{g/mL}$ (1.7 μM), the dispersions were further diluted with Hepes buffer. The polyplexes were allowed to equilibrate for 30 min at room temperature prior to use.

For FFS measurements on the pLL/ON complexes, 500 μL of the dispersion was prepared as described above, however, the final ONs concentration equaled 0.2 $\mu\text{g/mL}$ (34 nM). The φ of the pLL/ON complexes investigated by FFS equaled 20. After preparation, 200 μL of the sample was immediately transferred into the Nunc cuvettes (see below) to begin the FFS measurement.

The charge ratio (φ), i.e., the ratio of the number of positive charges on the pLL chains to the number of negative charges on the ONs, was calculated assuming that 1 μg of 20-mer ONs contained 3.43 nmol negative charges and that 1 μg of pLL contained 7.81 nmol positive charges, as calculated from the molecular weight of lysine monomer, the pK_a of lysine, and the pH of the solutions.

Particle Size Measurements. Dynamic light scattering measurements (DLS) on the pLL/ON polyplexes were carried out on a Malvern 4700 instrument (Malvern, Worcestershire, U.K.) at 25 $^{\circ}\text{C}$ and at an angle of 90 $^{\circ}$. The incident beam was a HeNe laser beam (633 nm). The polyplexes were prepared as described above. To avoid dust particles, the polymer solutions were filtered before being added to the nucleotide solutions. Average pore size of the filter was 0.45 μm (Schleicher & Schuell, Dassel, Germany). The particle size was measured 30 min after the preparation of the complexes. For calculating the z -average hydrodynamic diameter from the DLS data, the viscosity and refractive index of water at 25 $^{\circ}\text{C}$ (0.89 mPa·s and 1.333, respectively) were used. Polystyrene nanospheres (220 \pm 6 nm; Duke Scientific Corp, Palo Alto, CA) were used to verify the performance of the instrument. The particle size of each dispersion was measured three times.

ζ Potential Measurements. ζ potential measurements on the pLL/ON polyplexes were performed at 25 $^{\circ}\text{C}$ on a Malvern Zetasizer 2000 (Malvern, Worcestershire, U.K.), which is based on electrophoretic light scattering. ζ was measured within 1 h after the preparation of the complexes. Polystyrene nanospheres (-50 mV; Duke Scientific Corp, Palo Alto, CA) were used to verify the performance of the instrument. ζ of each dispersion was measured three times.

Fluorescence Fluctuation Spectroscopy (FFS). As explained in the Introduction, FFS basically monitors fluorescence intensity fluctuations in the excitation volume of a microscope. In dual-color FFS, both interacting components are labeled with spectrally different fluorophores (e.g., red and green) and their emission light is detected separately by two detectors monitoring the same excitation volume (Figure 1A). When dissociated, the components are only detected in one detector, as they carry a red or a green fluorophore. However, when associated, the complex is detected in both detectors *simultaneously* as it bears both red and green fluorophores. Autocorrelation analysis of the fluorescence fluctuations recorded in the green detector describes the diffusion behavior of all molecules emitting green light, regardless of whether they are free or associated with red-labeled components. On its turn, autocorrelation analysis of the red detector signal describes the diffusion of all red-labeled molecules. However, cross-correlation analysis on the fluorescence fluctuations registered in the red and the green detector provides only information on the diffusion behavior of the dual labeled (i.e., interacting) molecules.²⁴ However, when the fluorescence quantum yield strongly increases upon binding or when several fluorescent labeled molecules associate, the fluores-

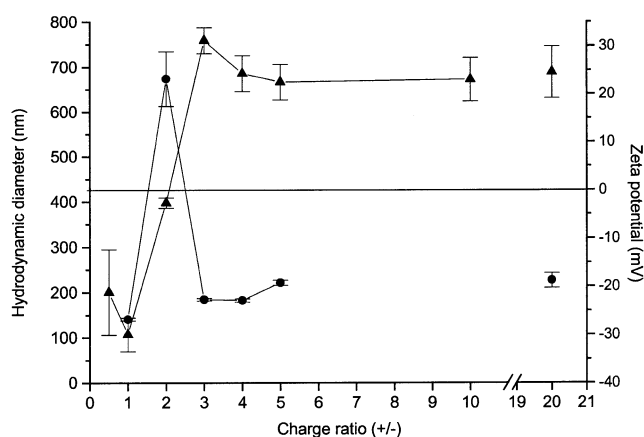


Figure 3. z -average hydrodynamic diameter (●) and ζ potential (▲) of pLL/ON complexes, as a function of the charge ratio. Each dispersion was measured three times.

cence emitted by a complex becomes much higher than that of the free molecules. Highly intense fluorescence peaks appear in the fluctuation profiles (e.g., Figure 2C), and in more extreme cases, auto- and cross-correlation analysis are no longer feasible. Therefore, a statistical approach is considered to analyze the fluorescence fluctuation profiles when bursts of high fluorescence intensity occur. Here, a threshold level is calculated, above which all fluorescence values are identified as "highly intense fluorescence peaks".^{11,25} In dual-color FFS, the *simultaneous* appearance of a highly intense fluorescence peak in the red and green detector indicates that a complex bearing both many red as well as many green labels is passing through the excitation volume.

In this study, dual-color FFS experiments were performed on a dual-color FFS setup installed on a MRC1024 Bio-Rad confocal laser-scanning microscope.²⁶ An inverted microscope (Eclipse TE300D, Nikon) was used, which was equipped with a water immersion objective lens (Plan Apo 60X, NA 1.2, collar rim correction, Nikon). The 488 and 647 nm lines of the same krypton-argon laser (Biorad, Cheshire, U.K.) were used. The intensities of both excitation wavelengths were controlled independently from each other, using an acousto-optic tunable filter. (Opto-Electronique, St. Rémy Les Chevreuse, France). To check whether the detectors adequately detected the fluorescence fluctuations in the excitation volumes (i.e., to verify whether the excitation volumes and the detection volumes optimally overlapped), the system was optimized as described by Schwillie et al.¹⁸

The size of the overlapping detection volumes was calculated from autocorrelation measurements with RhGr solution and equaled 7.9 fL.¹⁸ To perform the FFS measurements, the laser beam was focused at about 100 μm above the bottom of the cuvettes (Nalge Nunc International, Naperville, IL), which contained the samples. Prior to use, the thickness of the bottom of the cuvette was measured using a micrometer and the collar rim correction was adjusted for. In each FFS experiment, the fluorescence fluctuations were measured during 50 s. Diffusion coefficients were calculated using the average diffusion time of at least 20 measurements. Each pLL/ONs dispersion (both the single as well as the dual labeled) was independently prepared three times and each preparation was measured at least 10 times. The fluorescence fluctuation profiles shown in Figures 4–6 were representative for the measurements done on the respective pLL/ON dispersions.

The measurements on the homemade FFS apparatus were confirmed by conducting the same experiments on a commercial instrument (Confocor II, Zeiss-Evotec, Jena, Germany).

Results and Discussion

Figure 3 shows the average size and ζ of the pLL/ON complexes. The dependence of the size and surface properties of the pLL/ON complexes on φ shows a

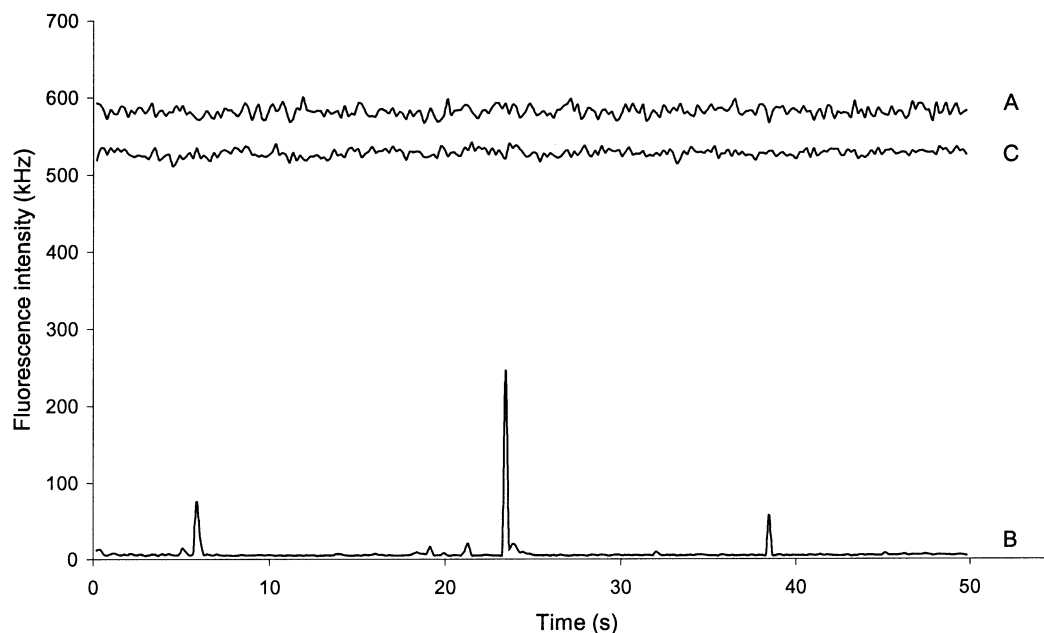


Figure 4. Fluorescence fluctuation profile, as measured by single-color FFS, of respectively a RhGr-ONs solution (A), a pLL/RhGr-ON dispersion (B, $\varphi = 20$), and the same dispersion after addition of dextran sulfate (C, final concentration of dextran sulfate equaled 12 $\mu\text{g/mL}$).

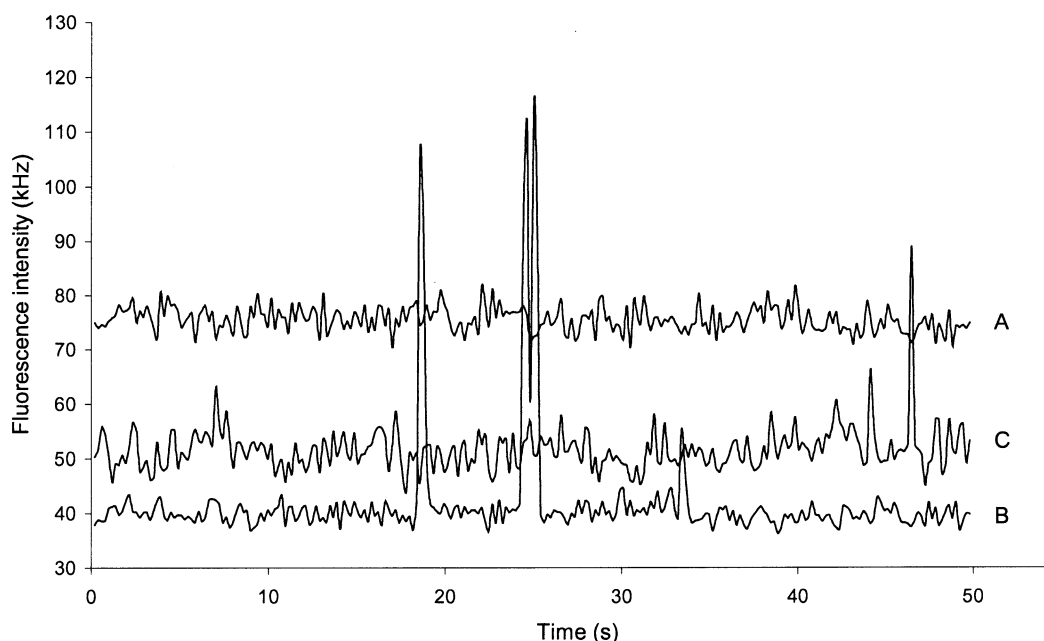


Figure 5. Fluorescence fluctuation profile, as measured by single-color FFS, of respectively a RhGr-pLL solution (A), a RhGr-pLL/ON dispersion (B, $\varphi = 20$), and the same RhGr-pLL/ON dispersion after addition of dextran sulfate (C, final concentration of dextran sulfate equaled 12 $\mu\text{g/mL}$).

typical profile as often observed for complexes formed between oppositely charged polyions.²⁷ At φ values between 1 and 3, large aggregates are formed. In this region, ζ equals approximately zero. Consequently, almost no electric repulsion occurs between the particles, which leads to a clustering of individual polyplexes. Upon further increasing the concentration of pLL, ζ reaches a plateau. The excess of cations in the complexes may explain the positive net charge of the polyplexes. This results in electric repulsion between the polyplexes, which prevents them from aggregating, and which explains the smaller size of the polyplexes at higher φ values in Figure 3.

Figure 4 (A data) shows the fluorescence fluctuation profile of free (i.e., noncomplexed) RhGr-ONs in buffer.

These data result in an autocorrelation function from which a diffusion coefficient of $(0.76 \pm 0.07) \times 10^{-6} \text{ cm}^2/\text{s}$ is calculated. This diffusion coefficient agrees with values reported in the literature.^{11,28}

The B data in Figure 4 show that the association of RhGr-ONs to pLL clearly influences the fluorescence fluctuation profile. Generally, the fluorescence intensity decreases. Moreover, highly intense fluorescence peaks also appear. The fluorescence intensity of the "baseline", originating from the presence of free RhGr-ONs in the excitation volume, decreases as most of the RhGr-ONs become associated with the pLL (schematically represented in Figure 1, parts B and C). This lowers the average number of free RhGr-ONs in the excitation volume. It is assumed that the highly intense fluores-

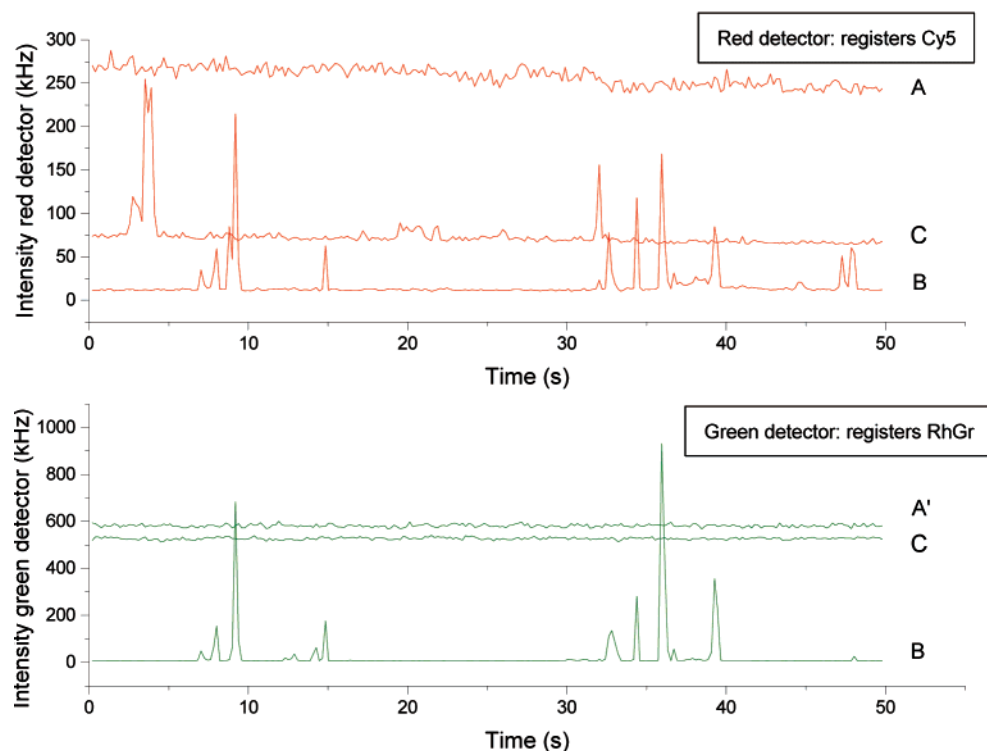


Figure 6. Fluorescence fluctuation profiles as *simultaneously* registered by the “red detector” (upper panel) and “green detector” (lower panel) of a Cy5-pLL/RhGr-ON dispersion ($\varphi = 20$) before (B) and after (C) addition of dextran sulfate. (A) and (A') are the fluorescence fluctuations of respectively a 2.0 $\mu\text{g/mL}$ (free) Cy5-pLL and a 0.2 $\mu\text{g/mL}$ (free) RhGr-ONs solution.

cence peaks originate from the presence of pLL chains that bear a large number of RhGr-ONs (Figure 1C). The distribution of the height of the peaks may be related to the polydispersity of the polyplexes with regard to the number of RhGr-ONs per polyplex. However, as the excitation profile in the confocal volume is not homogeneous and as single complexes do not necessarily always pass through the center of the focus, the fluorescence of a complex partly depends on the place where it moves through the excitation volume. Also, differences in the degree of mutual quenching of the fluorophores depending on their spatial proximity may influence the height of the highly intense fluorescence peaks. The highly intense fluorescence peak values disturb the calculation of an autocorrelation function from the fluorescence fluctuation profile.

Upon addition of dextran sulfate to the complexes (C data in Figure 4), the fluorescence intensity of the “baseline” is almost completely restored, while the highly intense fluorescence peaks disappear. Dextran sulfate is an anionic polymer, which competes with the RhGr-ONs for binding to the pLL chains. From the fluorescence fluctuations obtained after adding dextran sulfate, an autocorrelation curve can be derived, which yields a diffusion coefficient of $(0.77 \pm 0.06) \times 10^{-6} \text{ cm}^2/\text{s}$. This value corresponds to the diffusion coefficient as measured for free RhGr-ONs. The incomplete recovery of the fluorescence intensity of the baseline may be attributed to the adsorption of pLL/RhGr-ON complexes to the Eppendorf tubes. Especially since we have observed that the longer the incubation time of the polyplexes prior to addition of dextran sulfate, the lower the degree of recovery of the fluorescence intensity of the baseline after adding dextran sulfate (data not shown).

In a second series of experiments, the fluorescence fluctuation profiles of RhGr-pLL/ON complexes have

been measured (Figure 5). Contrary to the measurements in Figure 4, the polymer chains, instead of the ONs, are fluorescently labeled with RhGr. The diffusion coefficient of RhGr-pLL, as calculated from the autocorrelation analysis of the A data in Figure 5, equals $(1.5 \pm 0.2) \times 10^{-6} \text{ cm}^2/\text{s}$. The B data in Figure 5 show that, upon complexation of RhGr-pLL to ONs, highly intense fluorescence peaks appear and that the fluorescence intensity of the baseline significantly decreases, similar to the results in Figure 4. The highly intense fluorescence peaks in the B data of Figure 5 clearly show that a RhGr-pLL/ON complex consists of a number of RhGr-pLL chains. Combining the results of Figures 4 and 5 suggests that the pLL/ON complexes are “multimolecular”; i.e., they consist of a number of ONs associated with a number of pLL strands. However, these data cannot prove that *all* pLL/ON complexes are multimolecular.

Upon addition of dextran sulfate (C data in Figure 5), the fluorescence intensity of the baseline is only slightly restored. Also, the highly intense fluorescence peaks do not always disappear, indicating that structures carrying many RhGr-pLL chains continue to exist. Autocorrelation analysis of the fluctuations of the baseline between highly intense fluorescence peaks yields a diffusion coefficient that is 1 order of magnitude lower than the value obtained for the free RhGr-pLL solution. However, a reproducible diffusion coefficient has not been obtained. These phenomena are probably attributed to the binding of the dextran sulfate polyanion to positively charged RhGr-pLL chains, resulting in complexes that are heterogeneous in size. We therefore suggest that the highly intense fluorescence peaks that remain after adding dextran sulfate (C data in Figure 5) are RhGr-pLL/dextran sulfate complexes. Adding dextran sulfate to a sample of free RhGr-pLL indeed has supported this hypothesis, as a diffusion coefficient

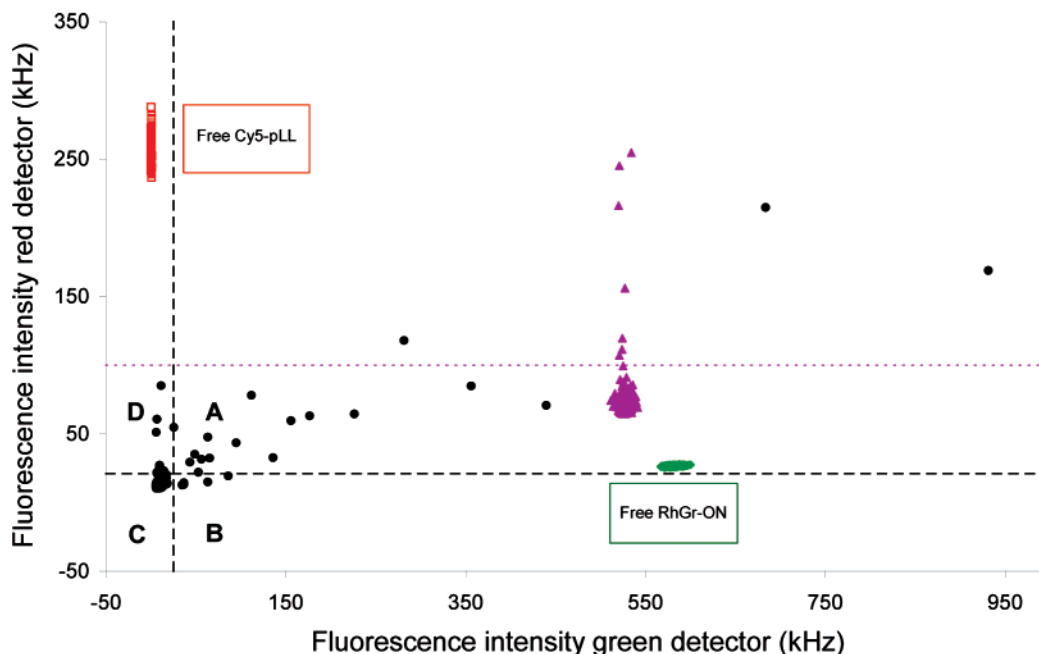


Figure 7. Scatter plot of the fluorescence fluctuations data, measured by dual-color FFS as represented in Figure 6, of free RhGr-ONs ($0.2 \mu\text{g/mL}$, \diamond), free Cy5-pLL ($2.0 \mu\text{g/mL}$, \square), and Cy5-pLL/RhGr-ON polyplexes before (\bullet) and after adding dextran sulfate (Δ).

of $(0.10 \pm 0.01) \times 10^{-6} \text{ cm}^2/\text{s}$, significantly lower than the diffusion coefficient of free RhGr-pLL (i.e., $(1.5 \pm 0.2) \times 10^{-6} \text{ cm}^2/\text{s}$), has been obtained.

Figure 5 shows that due to the association of the pLL to the dextran sulfate, highly intense fluorescence peaks remain in the fluorescence fluctuation profiles, although Figure 4 shows that the ONs are released from their cationic carrier. Similarly, upon dissociation of the polyplexes in the cell, the polymer and/or the ONs may unspecifically interact with different species which may result in highly intense fluorescence peaks when studied by single-color FFS. We propose that the fluorescent labeling of both the carrier and the ONs should improve the signal specificity. Therefore, in this study we have evaluated whether dual-color FFS allows studying the complexation between ONs and pLL. To minimize the detection of emission light from the green dye (i.e., RhGr) by the red detector, we have made use of RhGr and Cy5. It has been shown previously that the “cross-talk” between these fluorophores is limited, which makes them suitable for dual-color FFS.¹⁸ In the dual-color FFS experiments we have studied both RhGr-pLL/Cy5-ON complexes (data not shown) as well as Cy5-pLL/RhGr-ON complexes, which are discussed below.

Figure 6 shows the fluorescence fluctuations measured *at the same time* by the red (upper panel) and green (lower panel) detector. The A data (upper panel) represent the fluorescence fluctuation profile of free Cy5-pLL, whereas the A' data (lower panel) are the fluorescence fluctuations of free RhGr-ONs.

As the B data in Figure 6 show, the complexation of RhGr-ONs to Cy5-pLL decreases the fluorescence intensity of the baseline in both detectors. Moreover, highly intense fluorescence peaks also appear in both channels. It is especially clear that highly intense fluorescence peaks are registered by the two detectors at the same time. This means that at certain times a number of RhGr-ONs and a number of Cy5-pLL strands simultaneously move through the excitation volume. This proves that the pLL/ON complexes are indeed

multimolecular as already suggested from the single-color FFS results in Figures 4 and 5.

Upon addition of dextran sulfate, highly intense fluorescence peaks are no longer detected by the green detector (C data in the lower panel of Figure 6). Also, the fluorescence intensity of the baseline almost completely returns to the value observed for free RhGr-ONs. The diffusion coefficient, as calculated from the autocorrelation function, equals the one obtained for free RhGr-ONs, proving that RhGr-ONs are released from the polyplexes upon addition of dextran sulfate. All these observations completely agree with the results from the single-color FFS measurements on pLL/RhGr-ON complexes (Figure 4). Moreover, upon addition of dextran sulfate, the fluorescence intensity of the baseline as registered by the red detector is only partly restored, and highly intense fluorescence peaks remain present (C data in the upper panel of Figure 6). This again agrees with the single-color FFS observations on RhGr-pLL/ON complexes in Figure 5. Also, the diffusion coefficient calculated by autocorrelating the baseline fluorescence fluctuations between highly intense fluorescence peaks significantly differs from the diffusion coefficient of free Cy5-pLL. As suggested above, these phenomena are attributed to the binding of Cy5-pLL to dextran sulfate.

The fluorescence intensity profiles from Figure 6 are further analyzed in a two-dimensional scatter plot (Figure 7). Each data point in Figure 7 represents the green fluorescence (indicated by the x value) and red fluorescence (indicated by the y value) measured at a certain time in the excitation volume. First, the scatter plot shows the data obtained from the fluorescence fluctuation profiles measured in the red and green detector on free RhGr-ONs (\diamond) and on free Cy5-pLL (\square) solutions. Second, the \bullet -data are derived from the fluorescence fluctuation profiles, as measured by the red and green detector, on Cy5-pLL/RhGr-ON dispersion. Clearly, the \bullet -data at high x and y values originate from the highly intense fluorescence peaks in the B data of

Figure 6 and correspond to the multimolecular Cy5-pLL/RhGr-ON complexes. The ●-data at lower x and y values originate from the baseline in Figure 6 (B data) and correspond to structures bearing only one or a few Cy5-pLL strands and/or RhGr-ONs. To separate the multimolecular Cy5-pLL/RhGr-ON complexes efficiently in the ●-data, a "threshold value" is calculated by an algorithm that identifies the smallest outlier in the data set.²⁵ This threshold value, being the fluorescence intensity above which a fluorescence value is identified as a highly intense fluorescence peak, is determined for the fluorescence intensity profiles, registered by the green and red detector respectively, of the Cy5-pLL/RhGr-ON dispersion (B data in Figure 6). The horizontal dotted line (black) in Figure 7 shows the threshold value of the fluorescence fluctuations measurement by the red detector; the vertical dotted line (black) shows the one for the fluorescence fluctuations measured by the green detector. These lines divide the two-dimensional scatter plot in four quadrants and allow a more detailed evaluation of the distribution of the ●-data. The ●-data in quadrant A originate from complexes that simultaneously show a high fluorescent signal both in the red and green detector; these data are attributed to complexes that consist of many Cy5-pLL and many RhGr-ON molecules. The ●-data in quadrant B are Cy5-pLL/RhGr-ON complexes that contain numerous RhGr-ONs but only one or a few Cy5-pLL molecules. The ●-data in quadrant D are Cy5-pLL/RhGr-ON complexes that contain numerous Cy5-pLL chains but only one or a few RhGr-ONs. The ●-data in quadrant C do not originate at all from multimolecular complexes. They probably originate from structures carrying too little Cy5-pLL and RhGr-ON molecules to be identified as a peak of high fluorescence intensity.

After adding dextran sulfate, the data points of the Cy5-pLL/RhGr-ON sample (Δ) approach the x -position of the data points of the original RhGr-ON sample (◇) and only slight variations around the average x value of 530 kHz are observed. However, some of these data points have y values that differ significantly from the average y value around 70 kHz. This average y value of 70 kHz still is much lower than the 260 kHz of the original Cy5-pLL sample (□).

As only slight variations around the average x value are observed, the statistical algorithm is not able to identify any outliers in the set data points; hence, no threshold value can be calculated for the green detector. This means no peaks of high green fluorescence intensity are identified.

For the red detection channel, a threshold line can be calculated for the Cy5-pLL/RhGr-ON dispersion after adding dextran sulfate (horizontal dotted line (red) in Figure 7). Data points located above this threshold line are identified as peaks of high red fluorescence intensity and indicate that complexes bearing many Cy5-pLL strands still exist.

Summary and Conclusions

This paper shows that dual-color FFS is a straightforward method to detect the association and dissociation of pLL/ON complexes. The FFS results on the dual labeled polymer/oligonucleotide complexes match the observations seen in the single-color FFS measurements. Although we have not observed controversies between the single-color and dual-color FFS results on pLL/ON complexes, a clear disadvantage of dual-color

FFS is that both interacting species have to be labeled, which enhances the risk of fluorophore induced artifacts. However, the very sensitive detectors used in FFS permit attaching only one fluorescent marker per polymer chain, which may not substantially modify the properties of the macromolecules. As explained above, dual-color FFS is much more specific since aggregates of a single-color approach can be attributed to artificial environmental effects. In heterogeneous media like cells the DNA and the cationic polymers may interact not only with each other but also with many other different species. Furthermore, by two-dimensional scatter plot analysis of the dual-color FFS data, we have obtained a more detailed view on the composition of the pLL/ON complexes in the dispersion. It was shown that not all aggregates consist of numerous ONs bound to numerous pLL strands. Finally, both autocorrelation analysis and fluorescence fluctuation analysis suggest that the RhGr-ONs are released from the complexes after addition of dextran sulfate.

Acknowledgment. B.L. is a doctoral fellow of IWT. The financial support of this institute is acknowledged with gratitude. The Ghent University (UG-BOF) and FWO-Flanders (G.0310.02) supported this project through instrumentation credits and financial support. We are grateful to Prof. Dr. A. J. W. G. Visser and Dr. M. A. Hink (Wageningen Agricultural University, The Netherlands) for the use of the Confocor II and their advice. Dr. N. Opitz (Max Planck Institute for Molecular Physiology, Dortmund, Germany) is acknowledged for the installation of the FFS module on the MRC-1024 and for his dedicated support.

References and Notes

- (1) Stein, C. A.; Cheng, Y. C. *Science* **1993**, *261*, 1004–1012.
- (2) Elbashir, S. M.; Harborth, J.; Lendeckel, W.; Yalcin, A.; Weber, K.; Tuschl, T. *Nature (London)* **2001**, *411*, 494–498.
- (3) Gao, X.; Huang, L. *Gene Ther.* **1995**, *2*, 710–722.
- (4) De Smedt, S. C.; Demeester, J.; Hennink, W. E. *Pharm. Res.* **2000**, *17*, 113–126.
- (5) Felgner, P. L.; Barenholz, Y.; Behr, J. P.; Cheng, S. H.; Cullis, P.; Huang, L.; Jessee, J. A.; Seymour, L.; Szoka, F.; Thierry, A. R.; Wagner, E.; Wu, G. *Hum. Gene Ther.* **1997**, *8*, 511–512.
- (6) Zabner, J.; Fasbender, A. J.; Moninger, T.; Poellinger, K. A.; Welsh, M. J. *The J. Biol. Chem.* **1995**, *270*, 18997–19007.
- (7) Arigita, C.; Zuidam, N. J.; Crommelin, D. J. A.; Hennink, W. E. *Pharm. Res.* **1999**, *16*, 1534–1541.
- (8) Izumrudov, V. A.; Kargov, S. I.; Zhiryakova, M. V.; Zezin, A. B.; Kabanov, V. A. *Biopolymers* **1995**, *35*, 523–531.
- (9) Katayose, S.; Kataoka, K. *Bioconjugate Chem.* **1997**, *8*, 702–707.
- (10) Schwillie, P. *Cell Biochem. Biophys.* **2001**, *34*, 383–408.
- (11) Van Rompaey, E.; Sanders, N.; De Smedt, S. C.; Van Craenenbroeck, E.; Engelborghs, Y.; Demeester, J. *Macromolecules* **2000**, *33*, 8280–8288.
- (12) Van Rompaey, E.; Chen, Y.; Müller, J. D.; Gratton, E.; Van Craenenbroeck, E.; Engelborghs, Y.; De Smedt, S. C.; Demeester, J. *Biol. Chem.* **2001**, *382*, 379–386.
- (13) Van Rompaey, E.; Engelborghs, Y.; Sanders, N.; De Smedt, S. C.; Demeester, J. *Pharm. Res.* **2001**, *18*, 928–936.
- (14) Zelphati, O.; Szoka, F. C. *Proc. Natl. Acad. Sci. U.S.A.* **1996**, *93*, 11493–11498.
- (15) Marcusson, E. G.; Bhat, B.; Manoharan, M.; Bennett, C. F.; Dean, N. M. *Nucleic Acids Res.* **1998**, *26*, 2016–2023.
- (16) Godbey, W. T.; Wu, K. K.; Mikos, A. G. *Proc. Natl. Acad. Sci. U.S.A.* **1999**, *96*, 5177–5181.
- (17) Brock, R.; Jovin, T. M. *Cell. Mol. Biol. (Paris)* **1998**, *44*, 847–856.
- (18) Schwillie, P.; Meyer-Almes, F. J.; Rigler, R. *Biophys. J.* **1997**, *72*, 1878–1886.

- (19) Kettling, U.; Koltermann, A.; Schwille, P.; Eigen, M. *Proc. Natl. Acad. Sci. U.S.A.* **1998**, *95*, 1416–1420.
- (20) Koltermann, A.; Kettling, U.; Bieschke, J.; Winkler, T.; Eigen, M. *Proc. Natl. Acad. Sci. U.S.A.* **1998**, *95*, 1421–1426.
- (21) Bieschke, J.; Giese, A.; Schulz-Schaeffer, W.; Zerr, I.; Poser, S.; Eigen, M.; Kretzschmar, H. *Proc. Natl. Acad. Sci. U.S.A.* **2000**, *97*, 5468–5473.
- (22) Zauner, W.; Ogris, M.; Wagner, E. *Adv. Drug Delivery Rev.* **1998**, *30*, 97–113.
- (23) Snyder, S. L.; Sobocinski, P. Z. *Anal. Biochem.* **1975**, *14*, 284–288.
- (24) Heinze, K. G.; Koltermann, A.; Schwille, P. *PNAS* **2000**, *97*, 10377–10382.
- (25) Van Craenenbroeck, E.; Matthys, G.; Beirlant, J.; Engelborghs, Y. *J. Fluoresc.* **1999**, *9*, 325–331.
- (26) Opitz, N. *Cell. Mol. Biol. (Paris)* **2000**, *46*, 170.
- (27) Trinh, C. K.; Schnabel, W. *Macromol. Chem. Phys.* **1997**, *198*, 1319–1329.
- (28) Politz, J. C.; Browne, E. S.; Wolf, D. E.; Pederson, T. *Proc. Natl. Acad. Sci. U.S.A.* **1998**, *95*, 6043–6048.

MA0202383